RESEARCH ARTICLE

Mixed Optimization Approach for Low-Thrust Perturbed Rendezvous via Neural Networks

AN-YI HUANG[ID] AND TIAN-JIAO ZHANG
State Key Laboratory of Astronautic Dynamics, Xi'an Satellite Control Center, Xi'an 710043, China

Corresponding author: An-Yi Huang (hay04@foxmail.com)

ABSTRACT This study proposes a new model to combine the advantages of the indirect method, neural network, and evolutionary algorithm for the optimization of long-duration, low-thrust orbit rendezvous problems in low Earth orbits. The strategy of dividing the trajectory into three stages with fixed laws of thrust (the second stage keeps coasting without thrust) in the previous studies is inherited, in which the orbit changes of each stage are the decision variables and allocated evenly to each revolution. We derive a new simplified indirect method of the single-revolution transfer to replace the fixed-direction solution when evaluating the total velocity increment in the global optimization framework based on the differential evolution algorithm. Two neural networks are trained and applied to further accelerate the solving process. A correction algorithm for obtaining the trajectory and thrust laws of high-precision numerical dynamics is also proposed. The simulation results prove that the mixed model can obtain better solutions compared with previous methods because the simplified indirect method ensures the satisfaction of the first-order necessary condition. The neural networks can avoid the time-consuming shooting process of the indirect method and decrease the optimization time to less than 1 s. Moreover, the correction algorithm just requires five iteration steps to obtain the high-precision solution. The method can be applied for both approximate mission analysis and precise trajectory generation for orbit transfers in low Earth orbits.

INDEX TERMS Orbit rendezvous, mixed optimization, simplified indirect method, neural network.

I. INTRODUCTION

Electrical propulsion has been widely applied in space missions owing to its high efficiency [1], [2], [3], [4], [5], [6], [7]. The thrust level is limited by the power system of the spacecraft, which can result in long-duration orbit transfers. Optimization of such multi-revolution transfers is a challenging problem because the terminal states are highly sensitive to the bias of the initial conditions after long-duration propagation [8], [9], [10]. Furthermore, low-thrust trajectory calculation is also highly time-consuming when perturbations must be considered and significantly decreases the efficiency of the target-shooting process.

Extensive studies have been conducted for low-thrust trajectory optimization of the two-body dynamics [11], [12], [13], [14], [15], [16]. The multiple shooting method [15] and shape-based method [16] can be applied to overcome the

The associate editor coordinating the review of this manuscript and approving it for publication was Turgay Celik[ID].

difficulty in guessing initial values. The two-body optimal trajectory can then be considered an initial guess to solve the perturbed-orbit rendezvous problem by iterations [17], [18]. However, although such methods can correct the deviations caused by perturbations, they cannot actively use perturbations to change the orbit. In low-Earth orbits (LEOs), the time-varying drifts of the right ascension of the ascending node (RAAN) and the argument of perigee caused by J_2 perturbation must be included in optimization [19]. The RAAN difference between two orbits may continue increasing and thus lead to a failure of iteration that begins with the two-body solution.

On the contrary, the spacecraft can be allowed to go to an intermediate orbit of a certain drift rate and change its RAAN indirectly [5], [9], [20], [21], [22], [23], [24]. Huang et al. [9] proposed an approximate method to evaluate the optimal fuel consumption, and Wijayatunga et al. [5] proposed an approximate guidance calculation for low-thrust transfers. Such approximations can be applied in the optimization

of a multi-debris removal mission. Cerf [20] derived the optimal transfer trajectory between circular orbits by the minimal principle using a three-stage assumption including natural RAAN drift; Wen et al. [21] further improved on this approach by using a yaw-switch strategy. Huang et al. [22] and Shen [23] constructed equality constraint optimization models by simplifying the effect of thrust to approximate the expression of orbital elements, thus significantly reducing the calculation burden. Casalino and Andrea [24] also studied the trajectory optimization that actively uses both J_2 perturbation and atmospheric drag. These methods can be applied only to circular orbits, and are not sufficiently practical for transfers in LEO constellations or debris clusters. Huang and Li [25] recently proposed a parametric optimization model for low-eccentricity orbit rendezvous, which also included a correction process to obtain a high-precision trajectory. This method assumes the direction of thrust to be fixed to reduce the complexity and thus leads to loss of thrust efficiency when the thrust arc in each revolution is long. Recently, the deep neural network has been widely applied in space trajectory optimization of landing problem [26], [27], [28], asteroid exploration [29], [30] or transfers in the Earth orbits [31], [32]. However, directly constructing a neural network for the approximation of multi-revolution low-thrust transfers in LEOs is difficult. Because the revolution number is over hundreds and the influence of J_2 perturbation is considerable, current optimization methods cannot ensure obtaining the global optimal solutions when sampling the training data. A lot of local optimal solutions in the training data may greatly decrease the precision. Therefore, this study would find a new method to combine the advantages of neural networks and evolutionary algorithms.

This study conducts a follow-up study of Huang's original work in [25], proposing a novel mixed trajectory optimization model for low-thrust perturbed-orbit rendezvous in low-eccentricity orbits. The global optimization framework by dividing the trajectory into three stages that follow respective laws of thrust (the second stage keeps coasting without thrust) is inherited. The difference is that a simplified indirect method to obtain the optimal law of thrust of a single revolution with given changes in orbital elements is proposed to replace the sub-boundary value problem with fixed-direction thrust in [25], and two neural networks for quickly obtaining the feasibility and evaluating the thrust-on time are trained to further improve the efficiency. The simplifications in the optimization can greatly improve the efficiency but bring errors between the simplified model and the high-precision dynamic model. Thus, a new correction process for obtaining the high-precision trajectory and thrust laws is also proposed.

Compared with [25], the mixed method in this study requires less velocity increment for the same transfer, especially when the ratio of thrust is great (close to full thrust) because the thrust law obtained by the simplified indirect method is more efficient than the fixed-direction strategy. Compared with previous indirect methods directly used for

multi-revolution transfers, the indirect method in this study is just applied for a single revolution, which is easier to solve and can avoid obtaining local optimal solutions with different revolutions (which can be observed in [33], [34], and [35]). Compared with methods to directly train neural networks for multi-revolution transfers, the neural networks for single-revolution transfer are easier to train and the inputs can be scaled to adapt to different thrust accelerations. Moreover, since the optimal law of thrust is expressed by the phase angle, it can be substituted to the numerical dynamics model to obtain a high-precision trajectory via a modified correction procedure.

The rest of this study is organized as follows. Section II describes the problem and the optimization model in [25]. Section III presents the simplified indirect method for single-revolution transfer and the corresponding neural network delegate models. The mixed optimization framework is also proposed in this section. Section IV gives numerical simulations for the training of the neural networks, the optimal trajectory by the mixed optimization model, and comparisons with previous works. Finally, Section V draws the conclusions.

II. PROBLEM DESCRIPTION AND BASIC ASSUMPTIONS

The focus of this study is the time-fixed fuel-optimal orbit-rendezvous problem for LEOs with low eccentricity, which is often encountered in orbit transfers between satellites in the same constellation or objects in the same debris cluster. The dynamics equations of a spacecraft with low-thrust electrical propulsion [25] are:

$$
\begin{cases}
\dfrac{da}{dt} = \dfrac{2}{n\sqrt{1-e^2}}[(\alpha_r + \alpha_r^p)e\sin f + (\alpha_t + \alpha_t^p)(1 + e\cos f)] \\[2mm]
\dfrac{de}{dt} = \dfrac{\sqrt{1-e^2}}{na}[(\alpha_r + \alpha_r^p)\sin f + (\alpha_t + \alpha_t^p)(\cos E + \cos f)] \\[2mm]
\dfrac{di}{dt} = \dfrac{r\cos u}{na\sqrt{1-e^2}}(\alpha_n + \alpha_n^p) \\[2mm]
\dfrac{d\Omega}{dt} = \dfrac{r\sin u}{na\sqrt{1-e^2}\sin i}(\alpha_n + \alpha_n^p) \\[2mm]
\dfrac{d\omega}{dt} = \dfrac{\sqrt{1-e^2}}{nae}[-(\alpha_r + \alpha_r^p)\cos f + (\alpha_t + \alpha_t^p)(1 + \dfrac{r}{p})\sin f] \\[2mm]
\quad - \cos i\dfrac{d\Omega}{dt} \\[2mm]
\dfrac{dM}{dt} = n - \dfrac{1-e^2}{nae}[(\alpha_r + \alpha_r^p)(2e\dfrac{r}{p} - \cos f) \\[2mm]
\quad + (\alpha_t + \alpha_t^p)(1 + \dfrac{r}{p})\sin f]
\end{cases}
\tag{1}
$$

where a, e, i, Ω, ω, and M are the classical orbital elements of spacecraft, f is the true anomaly, $p = a(1 - e^2)$ is the semi-latus rectum, u is the argument of latitude (also called the phase angle), and $n = \sqrt{\mu/a^3}$ is the orbital angular velocity. Note that when the eccentricity is very close to zero, the dynamic equations based on the position and velocity [9] should be used instead. $a^p = [\alpha_t^p, \alpha_n^p, \alpha_r^p]$ are the three acceleration components of perturbations in the local
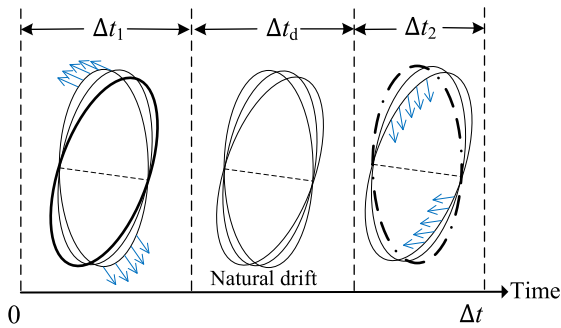
FIGURE 1. The three-stage orbit rendezvous strategy.

vertical/local horizontal reference frame(r: oriented in the direction of the position, n: the orbit normal, t: Perpendicular to r and n). α_t, α_n, and α_r are the three components of thrust acceleration a:

$$a = \begin{bmatrix} \alpha_t \\ \alpha_n \\ \alpha_r \end{bmatrix} = c(t)\alpha_{\max} \begin{bmatrix} f_t \\ f_n \\ f_r \end{bmatrix} \qquad (2)$$

where α_{max} is the max acceleration (in this paper it's assumed the mass change is negligible compared with the initial mass), $c(t) \in [0, 1]$ is a time-varying coefficient to represent the actual magnitude of acceleration (0 implies off and 1 implies full thrust), and $[f_t, f_n, f_r]^T$ is a normalized vector to represent the direction of the thrust.

The time-fixed orbit rendezvous problem can be expressed as follows. The initial orbit of the spacecraft is fixed to $[a_0, i_0, \Omega_0, e_{x0}, e_{y_0}, u_0]$ using the first class of nonsingular orbital elements, the target orbit is $[a_f, i_f, \Omega_f, e_{xf}, e_{yf}, u_f]$, and the transfer duration is fixed to Δt. The optimization task is to find the optimal law of thrust (including the direction and magnitude of thrust) to minimize the fuel consumption function J:

$$J = \int_0^{\Delta t} c(t)\dot{m}dt \qquad (3)$$

where $\dot{m}$ is the mass flow rate when the thrust is on.

For the orbits in a debris cluster or constellation, their differences in semimajor axis, inclination, and eccentricity are close to zero. The major aim of velocity increment is to eliminate the RAAN difference. Thus, as explained and validated in [20], [21], [22], and [23], when calculating the changes in orbital elements caused by thrust, the orbit can be treated as a circular orbit and the coupling terms in (1) are neglected. From these assumptions, Huang and Li [25] formed a parametric optimization model. The method includes two levels to obtain a solution closer to the global optimal solution of the time-fixed low-thrust rendezvous problem and retain high efficiency. First, the trajectory is assumed to be divided into three stages, as illustrated in Fig. 1 (Δt is the fixed transfer duration, Δt_1, Δt_d, Δt_2 are the duration of each stage).

The durations (Δt_1, Δt_2) and the direct changes in orbital elements $\Delta\sigma_i(\Delta a_1, \Delta i_1, \Delta\Omega_1, \Delta e_{x1}, \Delta e_{y1})$ by the thrust of

the first stage are decision variables. Then, the drift changes in RAAN, the argument of the perigee, and the argument of the latitude (u) can be analytically calculated using the orbit averaging theory [19]. The orbital elements should be converted to the mean elements [19] before being applied in (4) (the original elements in (1) are named the osculating elements):

$$\Delta\Omega_d = (\dot{\Omega}_d - \dot{\Omega}_0)(\Delta t - \frac{\Delta t_1}{2}) + (\dot{\Omega}_f - \dot{\Omega}_d)(\Delta t_2 - \frac{\Delta t_2}{2})$$
$$\Delta\omega_d = (\dot{\omega}_d - \dot{\omega}_0)(\Delta t - \frac{\Delta t_1}{2}) + (\dot{\omega}_f - \dot{\omega}_d)(\Delta t_2 - \frac{\Delta t_2}{2})$$
$$\Delta u_d = (n_d - n_0)(\Delta t - \frac{\Delta t_1}{2}) + (n_f - n_d)(\Delta t_2 - \frac{\Delta t_2}{2})$$
$$\qquad (4)$$

where n is the mean orbital angular velocity, and the subscripts '0', 'd', and 'f' mean the parameters of the initial orbit, drift orbit, and target orbit, respectively.

The sum of the direct changes and drift changes should be equal to the orbit difference between the initial and target orbits at the rendezvous time, which forms the constraint equations [25]:

$$\Delta a_1 + \Delta a_2 = \Delta a_0$$
$$\Delta i_1 + \Delta i_2 = \Delta i_0$$
$$\Delta\Omega_1 + \Delta\Omega_2 + \Delta\Omega_d = \Delta\Omega_0$$
$$\Delta e_{x1}' + \Delta e_{x2} = \Delta e_{x0}$$
$$\Delta e_{y1}' + \Delta e_{y2} = \Delta e_{y0}$$
$$\Delta u_d = \Delta u_0 \qquad (5)$$

where Δa_2, Δi_2, $\Delta\Omega_2$, Δe_{x2}, Δe_{y2} and Δa_2,Δi_2,$\Delta\Omega_2$,Δe_{x2}, Δe_{y2} are the direct changes in orbital elements of the first and third stages, respectively. $\Delta e_{x1}'$, $\Delta e_{y1}'$ are the changes in the two components of eccentricity with the drift of ω considered:

$$\Delta e = \sqrt{e_{x1}^2 + e_{y1}^2}$$
$$u_e = arctan(e_{y1}, e_{x1})$$
$$\Delta e_{x1}' = \Delta e \cos(u_e + \Delta\omega_d)$$
$$\Delta e_{y1}' = \Delta e \sin(u_e + \Delta\omega_d) \qquad (6)$$

Then, η_1, k_{11}, k_{12}, β_1, ϕ_1, u_1 and η_2, k_{21}, k_{22}, β_2, ϕ_2, u_2 are defined as the thrust parameters of a single revolution in the first and third stages, which can be analytically solved for by the average orbital changes in one revolution [25].

When the decision variables Δt_1, Δt_2, η_1, k_{11}, k_{12}, β_1, ϕ_1, u_1 are given, Δa_1, Δi_1, $\Delta\Omega_1$, Δe_{x1}, Δe_{y1}, $\Delta\Omega_d$, $\Delta\omega_d$, Δu_d and the thrust-on time of the first stage are known and Δa_2, Δi_2, $\Delta\Omega_2$, Δe_{x2}, Δe_{y2} are solved. Then, the thrust parameters of the third stage η_2, k_{21}, k_{22}, β_2, ϕ_2, u_2 are solved and the thrust-on time is obtained.

Finally, using the total thrust-on time as the objective function, a differential evolution (DE) algorithm [36] is applied to search for the best decision variables. A correction algorithm is also proposed in [25] to help obtain the trajectory of high-precision by a few iterations.

As analyzed in the following simulation results, when the thrust is nearly fully on, there will be a significant efficiency loss of the fixed-direction strategy because the thrust is assumed to be expansions of two impulses in each revolution. Therefore, we applied a simplified indirect method to obtain the optimal single-revolution solution to replace the strategy in [25] with a fixed thrust direction. The method is detailed in Section III.

III. MIXED OPTIMIZATION METHOD

In this section, the simplified indirect method is first proposed to replace the sub-boundary value problem of fixed-direction thrust. To further improve the efficiency of feasibility evaluation and thrust time calculation, two neural networks with the same input and hidden layers are trained by the results of the simplified indirect method. The new optimization framework modified by that in [25] is then proposed together with the correction process with high-precision numerical dynamics equations.

A. SIMPLIFIED INDIRECT METHOD FOR LOW-THRUST SINGLE-REVOLUTION TRANSFER

This section describes the relationship between the fixed-orbit element changes in semimajor axis, inclination, RAAN, and eccentricity vector ($\Delta \sigma = [\Delta a, \Delta i, \Delta \Omega, \Delta e_x, \Delta e_y]$) and the optimal law of thrust in one revolution by the indirect method. Note that in this section, $\Delta \sigma$ is the direct change by thrust. The change in u and the effect of perturbation will be considered in the next section. Indirect methods transform the optimal control problem into a boundary value problem by the minimal principle, which can be solved by nonlinear iteration methods [33], [34], [35]. Unlike in previous studies, the model described here was simplified based on the assumptions discussed in Section II.

When the change in the semimajor axis is small, the angular velocity of the spacecraft can be assumed constant and the argument of latitude ($u \in [0, 2\pi]$, and $\frac{du}{dt} = n_0$) can be used as the independent variable instead of time ($t \in [0, T]$) to express the orbital motion in one revolution. According to (1), for a near-circular orbit without any perturbation, we can replace dt by du/n_0:

$$\begin{cases} \dfrac{da}{du} = \dfrac{2a_0 c f_t \alpha_{\max}}{n_0 V_0} \\ \dfrac{di}{du} = \dfrac{c f_n \alpha_{\max}}{n_0 V_0} \cos u \\ \dfrac{d\Omega}{du} = \dfrac{c f_n \alpha_{\max}}{n_0 V_0 \sin i_0} \sin u \\ \dfrac{de_x}{du} = \dfrac{c \alpha_{\max}}{n_0 V_0}(2 f_t \cos u + f_r \sin u) \\ \dfrac{de_y}{du} = \dfrac{c \alpha_{\max}}{n_0 V_0}(2 f_t \sin u - f_r \cos u) \end{cases} \quad (7)$$

where $[a, i, \Omega, e_x, e_y]$ are the orbital elements during the transfer, $e_x = e \cos \omega$ and $e_y = e \sin \omega$ are the two components of the eccentricity vector, and $u = \omega + M$ is the argument of the latitude. $V_0 = \sqrt{\mu/a_0}$ and $n_0 = \sqrt{\mu/a_0^3}$ are the mean velocity and mean angular velocity of the

spacecraft, respectively. a_0 and i_0 are the initial semimajor axis and inclination, respectively. c is the abbreviation of $c(t)$ or $c(u)$.

(3) can be also rewritten as (8), which denotes the ratio between the thrust-on arc and the whole revolution and is equivalent to the fuel consumption.

$$J = \frac{\int_0^{2\pi} c \, du}{2\pi} \quad (8)$$

The requirement for orbit rendezvous can be expressed as

$$\begin{cases} \int_0^{2\pi} \dfrac{da}{du} = \Delta a \\ \int_0^{2\pi} \dfrac{di}{du} = \Delta i \\ \int_0^{2\pi} \dfrac{d\Omega}{du} = \Delta \Omega \\ \int_0^{2\pi} \dfrac{de_x}{du} = \Delta e_x \\ \int_0^{2\pi} \dfrac{de_y}{du} = \Delta e_y \end{cases} \quad (9)$$

To solve this optimal control problem ((7) is the dynamics equation, (8) is the objective function, and (9) is the terminal constraint) when the changes in orbital elements of one revolution are given, one can first write the Hamilton function according to the minimum principle:

$$H = \lambda_0 c + \lambda_\sigma^T \dot{\sigma} \quad (10)$$

where $\dot{\sigma} = [\frac{da}{a_0 du}, \frac{di}{du}, \frac{d\Omega}{du}, \frac{de_x}{du}, \frac{de_y}{du}]$ indicates the derivatives of the orbital elements (the semimajor axis a has been nondimensionalized by a/a_0). $\lambda_\sigma = [\lambda_a, \lambda_i, \lambda_\Omega, \lambda_{e_x}, \lambda_{e_y}]$ is the Lagrange multiplier (also called costate variables) to be determined, and λ_0 is another multiplier [33] to normalize λ_σ (i.e., to make $\left| [\lambda_0, \lambda_a, \lambda_i, \lambda_\Omega, \lambda_{e_x}, \lambda_{e_y}] \right| = 1$).

Then, the optimal law of thrust should minimize H. According to (7) and (10), the items related to f_t, f_n, f_r can be summarized as

$$\frac{c\alpha_{\max}}{n_0 V_0} \begin{bmatrix} 2\lambda_a + 2\cos u \lambda_{ex} + 2\sin u \lambda_{ey} \\ \cos u \lambda_i + \frac{\sin u}{\sin i_0}\lambda_\Omega \\ \sin u \lambda_{ex} - \cos u \lambda_{ey} \end{bmatrix}^T \begin{bmatrix} f_t \\ f_n \\ f_r \end{bmatrix} \quad (11)$$

Let $f = [f_t, f_n, f_r]^T$ denote the thrust direction. To minimize H, f should always be

$$f = -\frac{s}{\|s\|} \quad (12)$$

where $s = \begin{bmatrix} 2\lambda_a + 2\cos u \lambda_{ex} + 2\sin u \lambda_{ey} \\ \cos u \lambda_i + \frac{\sin u}{\sin i_0}\lambda_\Omega \\ \sin u \lambda_{ex} - \cos u \lambda_{ey} \end{bmatrix}$, and thus H is

$$H = (\lambda_0 - \frac{\alpha_{\max}\|s\|}{n_0 V_0})c \quad (13)$$

Because the range of c is [0, 1], to minimize H, c depends only on the value of $\lambda_0 - \frac{\alpha_{\max}\|c\|}{n_0 V_0}$:

$$c = \begin{cases} 0, & \lambda_0 - \dfrac{\alpha_{\max}\|s\|}{n_0 V_0} \geq 0 \\ 1, & \lambda_0 - \dfrac{\alpha_{\max}\|s\|}{n_0 V_0} < 0 \end{cases} \quad (14)$$

Let $\rho = \lambda_0 - \frac{\alpha_{max}\|s\|}{n_0 V_0}$ denote the switch function [33]. (14) indicates that the thrust acceleration should be either the maximum value or zero, which is called Bang–Bang control. The equation for λ_σ is

$$\dot{\lambda}_\sigma = -\frac{\partial H}{\partial \sigma} = 0 \qquad (15)$$

which indicates that in the simplified single-revolution transfer, the covariant variables λ_σ are constant during the transfer. Therefore, the optimization model obtained by the indirect method includes six unknown parameters (λ_σ and λ_0) and six shooting equations:

$$\begin{cases} \int_0^{2\pi} \frac{da}{a_0} = \frac{\Delta a}{a_0} \\ \int_0^{2\pi} di = \Delta i \\ \int_0^{2\pi} d\Omega = \Delta\Omega \\ \int_0^{2\pi} de_x = \Delta e_x \\ \int_0^{2\pi} de_y = \Delta e_y \\ \left\| [\lambda_a \ \lambda_i \ \lambda_\Omega \ \lambda_{e_x} \ \lambda_{e_y} \ \lambda_0] \right\| = 1 \end{cases} \qquad (16)$$

In this way, the optimal control problem is transformed into a boundary value problem and can be solved with a traditional nonlinear solving package such as MinPack-1 [37]. When (16) is solved, the optimal law of thrust and the ratio of thrust-on time can be obtained as

$$\Delta t_{thrust} = \frac{T_0}{2\pi} \int_0^{2\pi} c\,du \qquad (17)$$

where T_0 is the period of the initial orbit and is assumed to be constant in (16). Notably, when $\Delta\sigma = [\Delta a, \Delta i, \Delta\Omega, \Delta e_x, \Delta e_y]$ is too large and exceeds the limit of thrust level, there is no solution of (16). This condition means that such a low-thrust transfer is infeasible.

In summary, when $\Delta\sigma = [\Delta a, o\Delta i, \Delta\Omega, \Delta e_x, \Delta e_y]$ is given, λ_σ and λ_0 can be solved using (16). When λ_σ and λ_0 are fixed, the changes in orbital elements can be calculated by applying (9). As explained in [33], when solving (16) by employing nonlinear algorithms, initial guesses of λ_σ and λ_0 are required. However, it is difficult to make appropriate initial guesses that can guarantee convergence. Although in this study the single-revolution problem was simplified, it is highly time-consuming to generate random guesses of λ_σ and λ_0 repetitively and use them in the shooting process. Therefore, as described in Section III-B, we developed a surrogate model by utilizing a neural network to avoid the shooting process and improve the efficiency.

B. NEURAL-NETWORK SURROGATE MODEL FOR SINGLE-REVOLUTION TRANSFER

Neural network technology, which has become increasingly popular in recent years, is typically applied to generate surrogate models by using massive existing data sets to approach the output of a complex system [38]. The simple structure is convenient for the trajectory optimization problems of fixed input dimension and the performance has been proved in
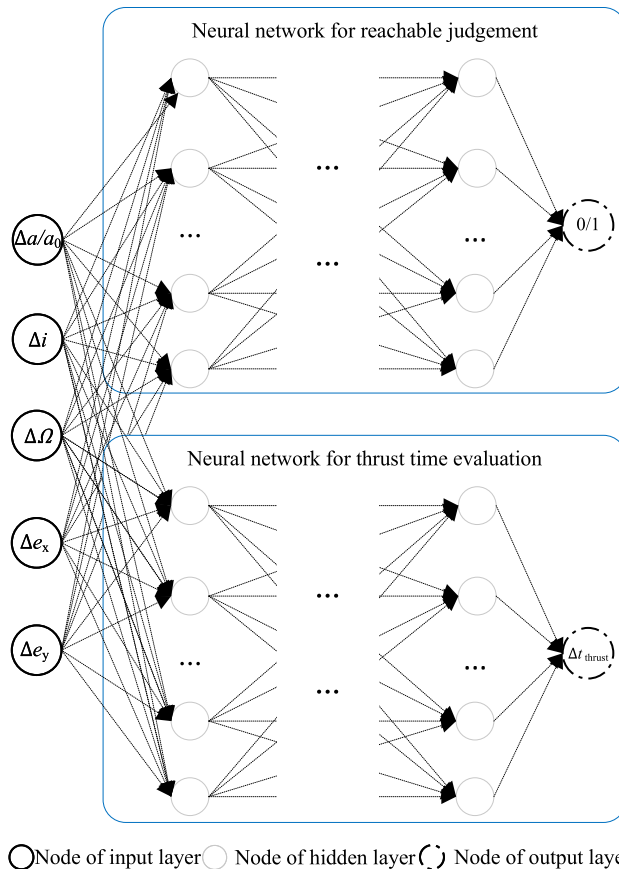

Node of input layer   Node of hidden layer   Node of output layer

FIGURE 2. Structure of two neural networks.

several existing studies [29], [30], [31], [32]. A typical neural network is composed of multiple layers, including an input layer, an output layer, and several hidden layers. In each layer, the input information is propagated to the next layer by nonlinear activation functions. In this study, two neural network surrogate models for single-revolution transfer were developed. One judges the feasibility of low-thrust transfer with given orbital changes, and the other evaluates the thrust time.

As discussed in Section III. A, the input layer of each neural network is five-dimensional (the orbital changes required for the spacecraft to complete the single revolution transfer: $\Delta a/a_0$, Δi, $\Delta\Omega$, Δe_x, Δe_y). The output of the first neural network is a Boolean variable (the input transfer is feasible or not) and the output of the second is a real number (the ratio of the thrust time to the transfer duration). The structure is illustrated in Fig. 2. The sampling data for training are generated as follows. Firstly, the range of each input variable should be determined to avoid invalid data. According to (7), when the thrust is always on and in the tangential direction, the maximum increment of the semimajor axis is

$$\Delta a_{max} = \frac{2\pi\alpha_{max}}{n_0 V_0} 2a_0 \qquad (18)$$
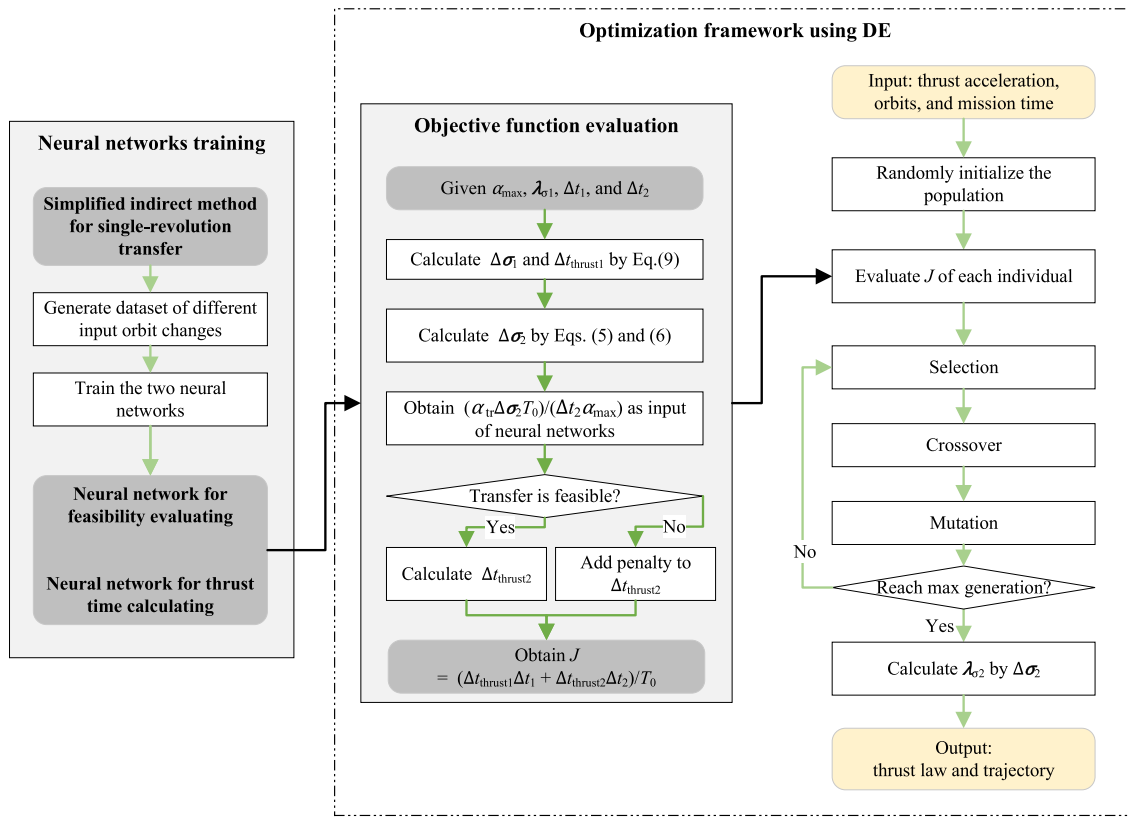
FIGURE 3. Flow chart of the mixed optimization.

Similarly, when the thrust is normal, the maximum changes in RAAN and inclination are

$$\begin{cases} \Delta i_{\max} = \frac{2\pi\alpha_{\max}}{n_0 V_0} \left| \frac{2\int_{-\pi/2}^{\pi/2} \cos u du}{2\pi} \right| = \frac{4\alpha_{\max}}{n_0 V_0} \\ \Delta\Omega_{\max} = \frac{2\pi\alpha_{\max}}{n_0 V_0 \sin i_0} \left| \frac{2\int_{-\pi/2}^{\pi/2} \cos u du}{2\pi} \right| = \frac{4\alpha_{\max}}{n_0 V_0 \sin i_0} \end{cases} \quad (19)$$

where $\left| \frac{2\int_{-\pi/2}^{\pi/2} \cos u du}{2\pi} \right| = \frac{2}{\pi}$ is the coefficient considering the superposition of orbit changes with different phases [22]. In addition, when the thrust is tangential but the directions within $u \in [0, \pi]$ and $u \in [\pi, 2\pi]$ are opposite, the changes in eccentricity are maximum:

$$\begin{cases} \Delta e_{x\max} = \frac{\Delta a_{\max}}{a} \frac{2}{\pi} = \frac{8\alpha_{\max}}{n_0 V_0} \\ \Delta e_{y\max} = \frac{\Delta a_{\max}}{a} \frac{2}{\pi} = \frac{8\alpha_{\max}}{n_0 V_0} \end{cases} \quad (20)$$

If any component in $\Delta\sigma = [\Delta a, \Delta i, \Delta\Omega, \Delta e_x, \Delta e_y]$ of a given transfer is over the ranges calculated by (18), (19), and (20), it can be directly obtained that the transfer is infeasible. Therefore, the training data need not include $\Delta\sigma$ over these ranges.

Secondly, a group of random vectors (five-dimensional real numbers within [-1, 1]) is generated to represent the input data of $\Delta\sigma$. Let $\{x_i\}$, $i = 1, 2, 3, 4, 5$ denote one of the vectors, the corresponding orbit changes are

$$[\Delta a, \Delta i, \Delta\Omega, \Delta e_x, \Delta e_y]$$

$$= [x_1 \Delta a_{\max}, x_2 \Delta i_{\max}, x_3 \Delta\Omega_{\max}, x_4 \Delta e_{x\max}, x_5 \Delta e_{y\max}] \quad (21)$$

Then, the indirect method described in Section III. A is applied to judge the feasibility and obtain the thrust-on time of each input vector. All the inputs and results subsequently form the sampling data set.

Finally, the sampling data set is divided into two parts, a training set and a testing set, to train the two neural networks shown in Fig. 2. In this study, Keras was employed to complete the training. Keras is a high-level open-source library built with Python for the neural network and deep learning. The details of Keras are provided in the literature [38].

In summary, the two neural networks use the same input to judge the feasibility of low-thrust transfer and evaluate the thrust time. It should be mentioned that when generating the sampling data, the thrust acceleration of the spacecraft is fixed (denoted by α_{tr}). When the actual acceleration is not equal to the fixed value, only a simple transformation is needed and there is no need to re-train the neural network.

According to (7), the optimal trajectory for another given acceleration $\alpha_{\max}$ and input $\Delta\sigma$ is equivalent to the trajectory for the fixed acceleration α_{tr} and input $\Delta\sigma_e = \alpha_{tr}\Delta\sigma/\alpha_{\max}$, where $\alpha_{tr}/\alpha_{\max}$ is the scale factor. Hence, the neural networks can be applied for different thrust levels after the training.
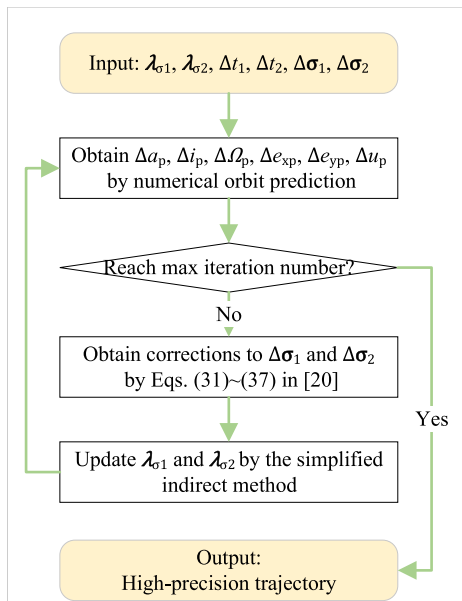
FIGURE 4. Flow chart of the correction process.

C. OPTIMIZATION FRAMEWORK USING DE

Using the neural network models, the framework in [25] can be modified to a mixed optimization model illustrated in Fig. 3. Firstly, the semimajor axis and inclination of the initial orbit are used in (7)∼(16) to generate a dataset of single-revolution transfers with different orbit changes and solve for the costate variables. The dataset is used to train the two neural networks. Then, for orbit rendezvous problems of similar semimajor axis and inclination, the neural networks are fixed and need not be re-trained. When the thrust acceleration α_{max}, initial and target orbits (used to calculate the orbit differences $\Delta\sigma$), and the transfer duration Δt of the problem are inputted, DE is applied to search for the optimal decision variables $(\lambda_{a1}, \lambda_{i1}, \lambda_{\Omega1}, \lambda_{e_{x1}}, \lambda_{e_{y1}}, \Delta t_1, \Delta t_2)$, in which the neural network based model is applied to evaluate the objective function of the population. DE is an efficient evolutionary algorithm for the optimization of continuous variables [36] and has also been well applied to trajectory optimization problems in [9] and [25]. Note that DE is not the focus of this paper and the proposed model is not highly dependent on the selection of the evolutionary algorithms. Other latest evolutionary algorithms can be also well applied.

In Fig. 3, $\alpha_{tr}\Delta\sigma_2 T_0/(\Delta t_2\alpha_{max})$ represent the average changes in one revolution of the third stage when the input acceleration α_{max} is different from the acceleration α_{tr} used for neural network training. The objective function is the sum of the thrust time of each stage by (17):

$$J = \Delta t_{thrust1}\frac{\Delta t_1}{T_0} + \Delta t_{thrust2}\frac{\Delta t_2}{T_0} \qquad (22)$$

where $\Delta t_{thrust1}$ and $\Delta t_{thrust2}$ represent the thrust times of a single revolution corresponding to the first and second stages, respectively, and $\frac{\Delta t_1}{T_0}$ and $\frac{\Delta t_2}{T_0}$ represent the revolution number

of the two stages. When DE converges, the optimal changes in orbit elements and thrust laws are obtained. The trajectory (time history of the orbital elements) based on the simplified dynamics ((7) and (4)) can also be obtained by combining the thrust determined by the optimal co-state variables ($\lambda_{\sigma1}$ and $\lambda_{\sigma2}$) and the analytical drifts by J_2 perturbation.

D. CORRECTION PROCESS USING HIGH-PRECISION DYNAMICS

The solution obtained by the process in Fig. 3 is approximate. This section proposes an iteration process to calculate the rendezvous trajectory with the high-precision numerical dynamic model. Since the law of thrust of each stage is expressed by the phase angle u using (9) and (11), when the numerical dynamic model is applied (a^p in (1) includes the perturbations such as the drag of the atmosphere, the high-order Earth's non-sphere model, the gravities of the sun and moon, and the solar radio pressure. The models are the same with [25]), and the trajectory can be obtained by three sequential numerical integrations ([0, Δt_1], [Δt_1, $\Delta t - \Delta t_2$], [$\Delta t - \Delta t_2$, Δt_2]). In the first and third stages, the phase angle u is obtained by the spacecraft's osculating orbit elements. In the second stage, the thrust is zero. In this way, the terminal orbit elements of the spacecraft are predicted.

However, there is a gap between them and the target orbit due to the difference in the dynamic equations. Let $\Delta\sigma_p = [\Delta a_p, \Delta i_p, \Delta\Omega_p, \Delta e_{xp}, \Delta e_{yp}, \Delta u_p]$ denote the orbit differences between the predicted orbit and actual target orbit. To obtain the thrust law that eliminates the differences, the correction algorithm in [25] is modified to the process illustrated in Fig. 4. The detail of calculating the correction terms to $\Delta\sigma_1$ and $\Delta\sigma_2$ by $\Delta\sigma_p$ is inherited. The difference is that in this study, updated $\Delta\sigma_1$ and $\Delta\sigma_2$ in each iteration step are used to update the thrust laws ($\lambda_{\sigma1}$ and $\lambda_{\sigma2}$) via the simplified indirect method instead of the fixed-direction solution in [25]. In this manner, the optimality of each revolution is guaranteed by the indirect method, and the global optimality of the transfer trajectory is guaranteed by searching for the orbital element changes via evolutionary algorithms.

IV. SIMULATION AND DISCUSSION

The test scenario is constructed as follows. The initial and target orbits of the spacecraft are detailed in Table 1. The thrust is 0.1 N, the initial mass is 500 kg, and the specific impulse is 2000 s (the power is about 1.5 kW). The required changes in orbital elements for rendezvous are $\Delta\sigma_0 = [\Delta a_0, \Delta i_0, \Delta\Omega_0, \Delta e_{x0}, \Delta e_{y0}, \Delta u_0] = [-45.443$ km, $-1.192°, -2.214°, -0.0046, 0.0096, 58.901°]$. Since the fuel flow rate is less than 5.1×10^{-6} kg/s, the thrust acceleration α_{max} is assumed to be constant ($2 \times 10^{-4} m/s^2$). We first trained the neural network surrogate models of single revolution transfer, then solved the mixed optimization model by DE, and finally obtained optimal trajectories of different thrust levels and compared them with previous methods.

TABLE 1. Initial orbits of the spacecraft and target.

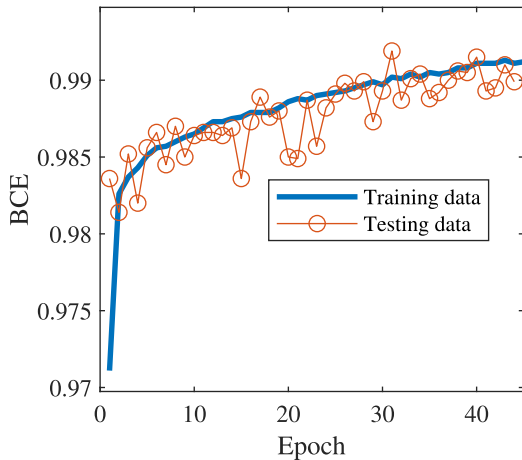|	Orbit	a (km)	e	i (°)	Ω (°)	ω (°)	M (°)
Initial	Osculating	7150.959	0.014111	98.6472	92.4174	194.397	50.8584
	Mean	7157.398	0.015212	98.6435	92.4211	197.619	47.5986
Target	Osculating	7102.877	0.005775	97.4559	98.1756	224.542	38.0186
	Mean	7111.954	0.007219	97.4512	98.1767	232.145	30.4031

FIGURE 5. Loss function (BCE) of the first neural network.
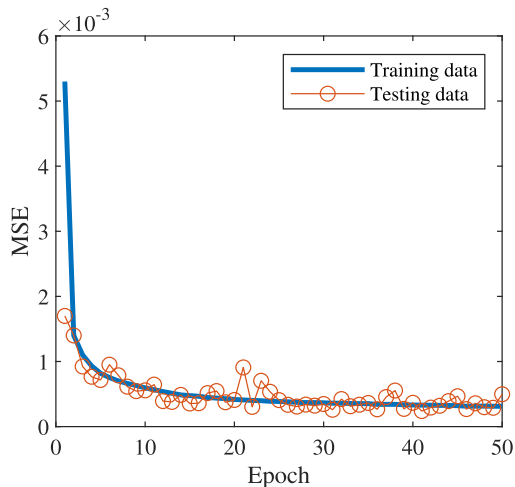

FIGURE 6. Loss function (MSE) of the second neural network.

A. NEURAL NETWORKS TRAINING PROCESS

The training data were generated as follows. The initial semimajor axis and inclination in (4) were set to $a_0 = 7157.398$ km, $i_0 = 98.6435°$, and $\alpha_{\max} = 2 \times 10^{-4} m/s^2$. Then, 300 000 random five-dimensional real number vectors within [-1, 1] were created to represent different single-revolution transfers by (18) $\sim$ (20) and used as input for the indirect optimization method to obtain the feasibility of each transfer and the corresponding thrust time. The transfer was recognized as infeasible when (16) failed to converge after 100 shooting iterations of randomly initial co-states. Finally, about 33,000 transfers were solved

successively. The average shooting number is about 40 and the convergence takes more than 20 seconds.

The structures and settings of the neural networks are detailed in Table 2. Cross-validation is applied by dividing the total data into ten subsets and using each of them as the validation set. The ten cases with different training sets and validation sets are tested separately and the loss functions after convergence are close. The results are shown in Table 3 and the histories of loss function are illustrated in Fig. 6 and Fig. 7. According to (3), the neural networks' outputs are not influenced when there are small biases of a_0 and i_0. It was validated that the outputs are acceptable (the mean BCE of the ten cases is greater than 0.99 and the mean MSE is less than 0.00031) when the bias of the semimajor axis and the inclination are within ± 200 km and $\pm 2°$, respectively. Obtaining the output of the trained neural networks takes less than 1×10^{-5} seconds, which is more efficient than the solving process of the indirect method. However, the training time (less than 1000 s) should be considered when new a_0 and i_0 are given and the neural networks need to be re-trained.

B. FUEL-OPTIMAL TRAJECTORY

The transfer duration was fixed to 30 days and the optimal trajectory was specified as follows. The duration of the first stage was 10.865 days, $[\Delta a_1, \Delta i_1, \Delta\Omega_1, \Delta e_{x1}, \Delta e_{y1}] = [-287.445$ km, $-0.1115°$, $0.4117°$, 0.00616, $0.000612]$, $[\lambda_{a1}, \lambda_{i1}, \lambda_{\Omega1}, \lambda_{e_{x1}}, \lambda_{e_{y1}}] = [0.400515, 0.15821, -0.52045, -0.05102, 0.01096]$, and the thrust-on time was 9.698 days. The duration of the second stage for free drifting was 3.403 days. The duration of the third stage was 15.732 days, $[\Delta a_2, \Delta i_2, \Delta\Omega_2, \Delta e_{x2}, \Delta e_{y2}] = [242.001$ km, $-1.0807°$, $0.398°$, -0.000874, $-0.00469]$, $\lambda_{a2}, \lambda_{i2}, \lambda_{\Omega2}, \lambda_{e_{x2}}, \lambda_{e_{y2}} = [-0.17226, 0.85444, -0.30873, -0.002031, 0.01701]$, and the thrust-on time was 14.199 days. The equivalent velocity increment was 412.95 m/s. To avoid directly changing RAAN by the cross-track thrust, the optimal trajectory firstly decreases the semimajor axis to less than 6900 km and restores it to the target semimajor axis at the third stage. By contrast, the method in [25] cannot obtain a feasible solution due to the efficiency loss of the fixed-direction strategy. The minimal thrust acceleration to complete the transfer of the proposed method is $1.8 \times 10^{-4} m/s^2$ yet that of the method in [25] is $2.9 \times 10^{-4} m/s^2$.

When the high-precision dynamics is applied (including the Earth's non-spherical gravitation of 20×20 order, the gravities of the sun and moon, the atmosphere drag, and the solar radial pressure, in which the spacecraft's area is

TABLE 2. Structures and parameter setting.

Parameters	Model 1 for feasibility judge	Model 2 for thrust time evaluation
Number of hidden layers	2	2
Number of nodes in hidden layer	60	60
Activate function of input & hidden layers	ReLU	ReLU
Activate function of output layer	Sigmod	NULL
Scale of training set	270000	30000
Scale of validation set	30000	3000
Loss function	BCE (Binary Cross Entropy)	MSE (Mean Square Error)

TABLE 3. Training results.

Results	Model 1 for feasibility judge	Model 2 for thrust time evaluation
Epochs of convergence	50	50
Training Time with 4.2 GHz CPU(s)	800	900
Loss on training set	0.99 (BCE)	0.00028 (MSE)
Loss on validation set	0.99 (BCE)	0.00031 (MSE)

TABLE 4. Orbit errors during the correction.

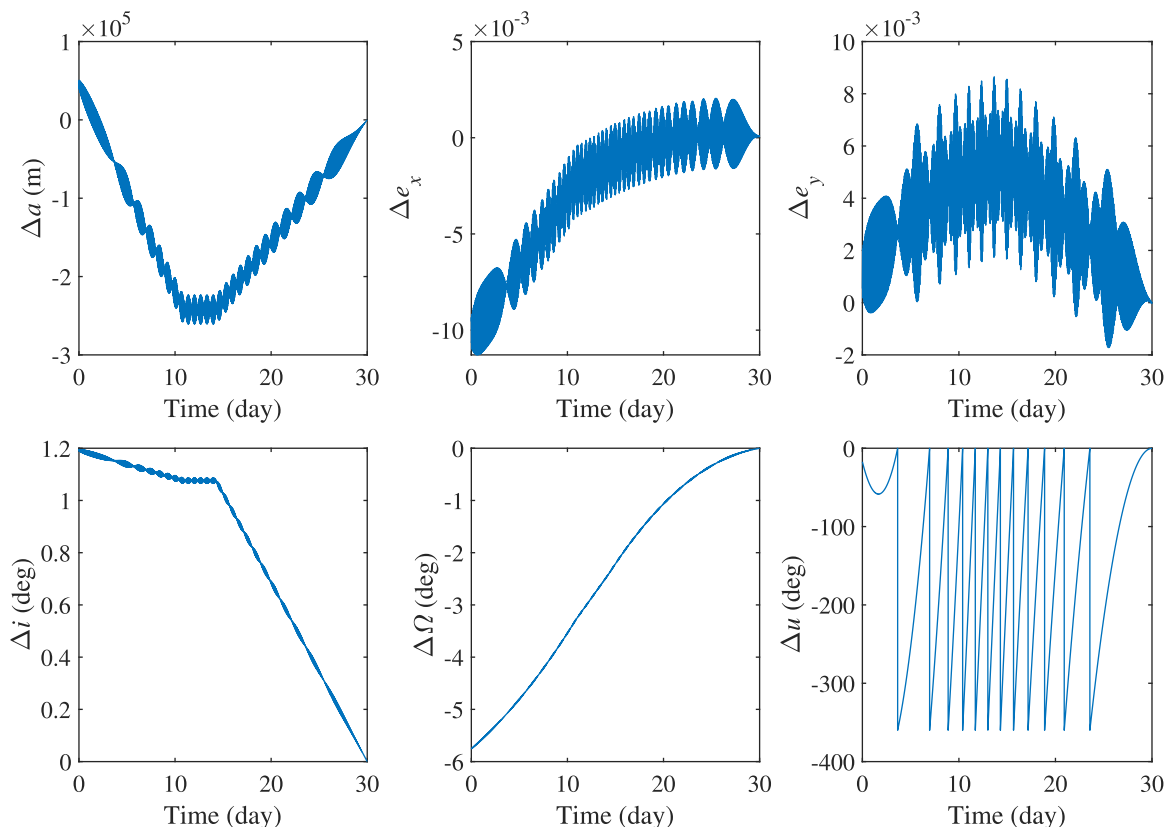| Step	Δa_p (km)	Δi_p (°)	$\Delta \Omega_p$ (°)	Δu_p (°)	Δe_{xp}	Δe_{yp}
No correction	3.035	-1.368E-02	1.425E-01	1.319E+02	-5.165E-04	6.152E-04
1	2.258	-2.544E-03	-7.724E-02	-8.911E+00	-2.580E-04	-2.825E-05
2	0.505	-2.387E-04	1.670E-02	1.385E+00	1.646E-05	2.592E-05
3	-0.037	-3.004E-05	-9.497E-04	-4.374E-01	-1.051E-05	-2.325E-06
4	0.017	-2.673E-06	5.779E-04	3.767E-02	3.568E-07	8.625E-07
5	-0.001	-1.084E-06	-4.407E-05	-1.773E-02	-3.825E-07	-1.485E-07

FIGURE 7. Histories of the orbital differences.

$6.0\,\mathrm{m}^2$, the drag coefficient is 2.2, and the solar radial pressure coefficient is 1.3), the corrected $[\lambda_{a1}, \lambda_{i1}, \lambda_{\Omega1}, \lambda_{ex1}, \lambda_{ey1}] =$ [0.4514, 0.1741, −0.6578, −0.1858, −0.01909] and $\lambda_{a2}, \lambda_{i2}, \lambda_{\Omega2}, \lambda_{ex2}, \lambda_{ey2}$ = [−0.1604, 0.8755, −0.3637,
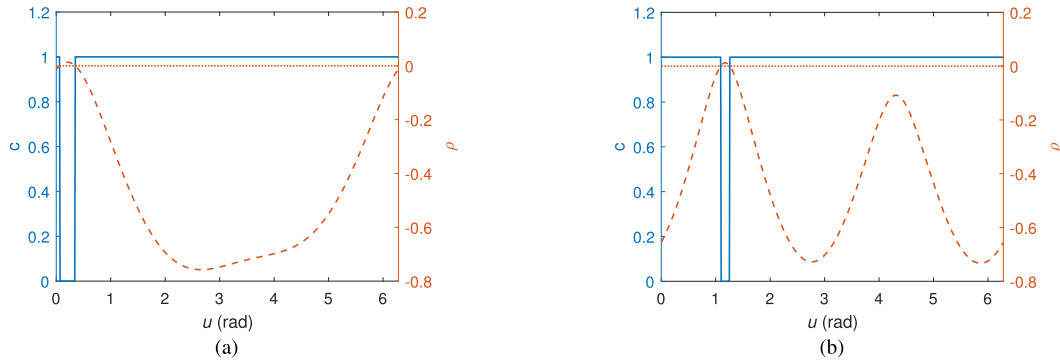
FIGURE 8. Optimal magnitude of thrust: (a) First stage, (b) Third stage.
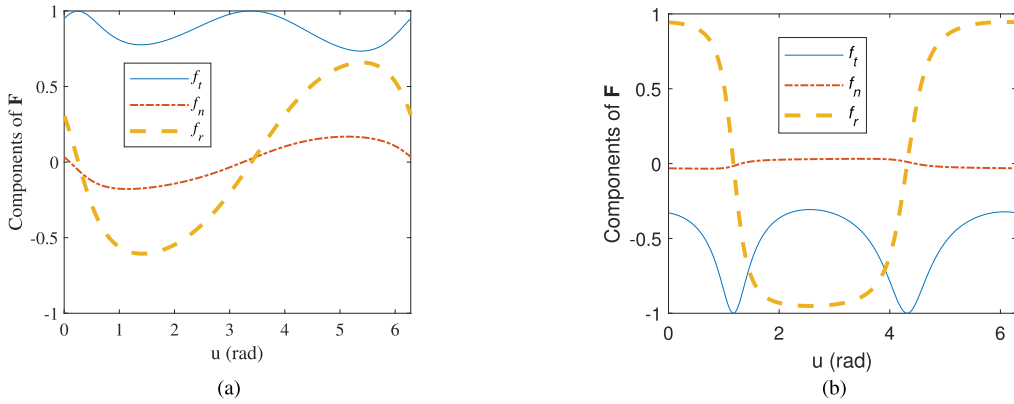

FIGURE 9. Optimal thrust direction: (a) First stage, (b) Third stage.

TABLE 5. Optimization results for different accelerations.

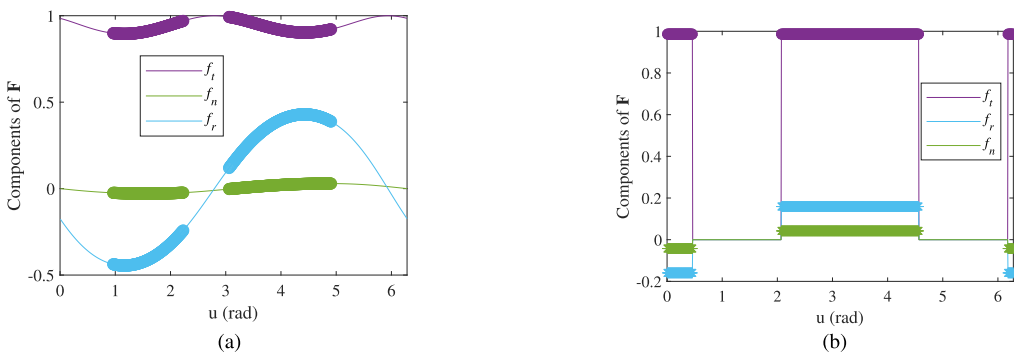| α_{max} ($10^{-4} m/s^2$)	Δv of the mixed method (m/s)	Δv of the method in [25] (m/s)
8	270.67	272.52
6	282.94	284.96
4	307.53	313.15
2.9	335.84	355.01
1.8	448.90	Infeasible

FIGURE 10. Thrust direction of the first stage: (a) Mixed model, (b) Fixed-direction.

0.007780, 0.02937]. The errors between the prediction and target orbits during the iterative correction are detailed in Table 4. After 5 steps of corrections, the orbit difference

was neglectable and the final velocity increment was 443.67 m/s. The histories of orbit elements during the transfer are illustrated in Fig. 7, and the thrust laws of
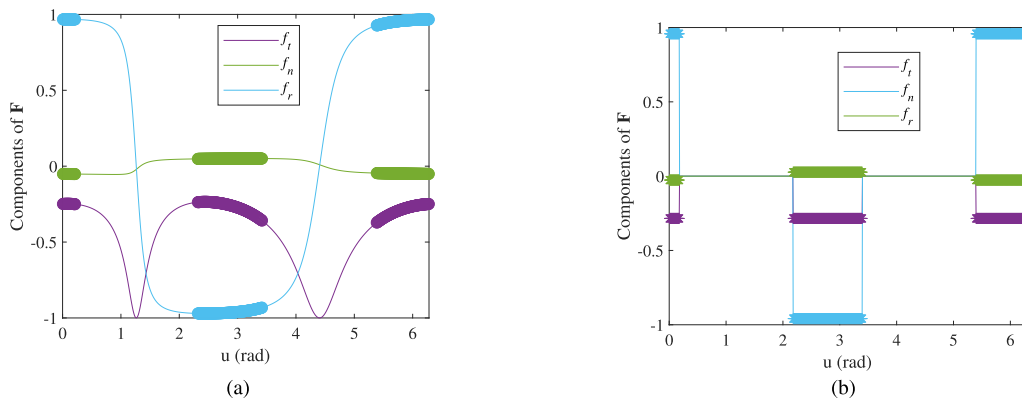
FIGURE 11. Thrust direction of the third stage: (a) Mixed model, (b) Fixed-direction.

the first and third stages are illustrated in Fig. 8 and Fig. 9.

C. TRAJECTORIES OF DIFFERENT THRUST LEVELS AND COMPARISON WITH PREVIOUS WORKS

The shooting of a single-revolution transfer in this study requires less than tens of repeating with random initial values, which is much easier than that of a many-revolution transfer in previous indirect methods (more than hundreds of shooting). Therefore, the proposed mixed model can quickly obtain the global solution. The advantages in convergence efficiency and optimality of the three-stage strategy compared with previous methods for low-thrust perturbed orbit rendezvous have been also proved in [25]. The calculation time of the proposed method is less than 1s (when a high-precision trajectory is required, each correction step takes 1 more seconds), which is close to the method in [25] because the upper-level DE algorithms of the two methods are similar. Therefore, we just compare the two methods' fuel cost (velocity increment).

When the thrust acceleration α_{max} is not equal to 2×10^{-4} m/s^2, as discussed in Section III-B, the input orbit differences should be pretreated by a multiplying factor $0.0002/\alpha_{max}$ to apply the neural networks. When $\alpha_{max} = 2.9 \times 10^{-4}$ m/s^2 (the minimal acceleration for feasible rendezvous using the method in [25]), our method obtained a solution of 335.84 m/s and the method in [25] requires 355.01 m/s. Different thrust accelerations were also tested and detailed in Table 5. It's proved the mixed model with the single-revolution indirect method requires less thrust-on time.

When $\alpha_{max} = 8 \times 10^{-4}$ m/s^2, the optimal thrust directions of the proposed method and the fixed-direction strategy in [25] are illustrated in Fig. 10 and Fig. 11 (the durations of each stage by the two methods are equal). In the third stage, the thrust ratio is less than 0.35 and the fixed-direction solution is close to the single-revolution indirect method because higher thrust acceleration results in easier transfer to the middle drift orbit, and a shorter thrust arc is closer to the extension of an impulse. However, in the first stage, the

thrust ratio is greater than 0.5, and thus the thrust directions obtained by the two methods are a little different.

V. CONCLUSION

The optimization of low-thrust time-fixed perturbed-orbit rendezvous in LEO is studied and a novel mixed approach based on neural networks and indirect method is proposed. The three-stage transfer strategy to use the natural drift of RAAN is inherited and the optimization framework of [25] is improved by replacing the fixed-direction strategy with the simplified indirect method when solving the thrust law of the single-revolution transfer. The efficiency is further improved by training two neural network surrogate models to check the feasibility of a transfer and evaluate the thrust time. The simulation results prove that the mixed model can obtain better trajectories compared with the method in [25]. The convergence efficiency and optimality of the mixed method compared with previous methods are guaranteed by the inherited DE-based framework, which has been proved in [25]. The neural networks just require a certain time for the training processes and then can be applied to avoid repeating the time-consuming shooting process of the indirect method. The time for obtaining the optimal trajectory is less than 1 s. The method can be applied to low-thrust trajectory optimization of missions such as active debris removal and in-orbit service. The proposed method assumed the semimajor axis and inclination are constant and the eccentricity is zero in the right function of (7), which are proved acceptable for obtaining high-precision trajectories between low-eccentricity and low-Earth orbits. When the changes in the semimajor axis and inclination are significant, the error would become not negligible. Future work will consider the continuously changing model for such orbit transfers.

REFERENCES
[1] C. Bonnal, J.-M. Ruault, and M.-C. Desjean, "Active debris removal: Recent progress and current trends," *Acta Astronautica*, vol. 85, pp. 51–60, Apr. 2013.

[2] L. Olivieri and A. Francesconi, "Large constellations assessment and optimization in LEO space debris environment," *Adv. Space Res.*, vol. 65, no. 1, pp. 351–363, Jan. 2020.

[3] A. Ruggiero, P. Pergola, and M. Andrenucci, "Small electric propulsion platform for active space debris removal," *IEEE Trans. Plasma Sci.*, vol. 43, no. 12, pp. 4200–4209, Dec. 2015.

[4] M. Leomanni, G. Bianchini, A. Garulli, A. Giannitrapani, and R. Quartullo, "Orbit control techniques for space debris removal missions using electric propulsion," *J. Guid., Control, Dyn.*, vol. 43, no. 7, pp. 1259–1268, Jul. 2020.

[5] M. C. Wijayatunga, R. Armellin, H. Holt, L. Pirovano, and A. A. Lidtke, "Design and guidance of a multi-active debris removal mission," *Astrodynamics*, vol. 7, no. 4, pp. 383–399, Dec. 2023.

[6] G. Viavattene, E. Devereux, D. Snelling, N. Payne, S. Wokes, and M. Ceriotti, "Design of multiple space debris removal missions using machine learning," *Acta Astronautica*, vol. 193, pp. 277–286, Apr. 2022.

[7] S. Guo, W. Zhou, J. Zhang, F. Sun, and D. Yu, "Integrated constellation design and deployment method for a regional augmented navigation satellite system using piggyback launches," *Astrodynamics*, vol. 5, no. 1, pp. 49–60, Mar. 2021.

[8] D. Morante, M. Sanjurjo Rivo, and M. Soler, "A survey on low-thrust trajectory optimization approaches," *Aerospace*, vol. 8, no. 3, p. 88, Mar. 2021.

[9] A.-Y. Huang, Y.-Z. Luo, H.-N. Li, and S.-G. Wu, "Optimization of low-thrust multi-debris removal mission via an efficient approximation model of orbit rendezvous," *Proc. Inst. Mech. Eng., G, J. Aerosp. Eng.*, vol. 236, no. 14, pp. 3045–3056, Nov. 2022.

[10] G. Viavattene, E. Grustan-Gutierrez, and M. Ceriotti, "Multi-objective optimization of low-thrust propulsion systems for multi-target missions using ANNs," *Adv. Space Res.*, vol. 70, no. 8, pp. 2287–2301, Oct. 2022.

[11] T. N. Edelbaum, "Optimum low-thrust rendezvous and station keeping," *AIAA J.*, vol. 2, no. 7, pp. 1196–1201, Jul. 1964.

[12] Y. Gao, "Near-optimal very low-thrust earth-orbit transfers and guidance schemes," *J. Guid., Control, Dyn.*, vol. 30, no. 2, pp. 529–539, Mar. 2007.

[13] C. A. Kluever, "Simple guidance scheme for low-thrust orbit transfers," *J. Guid., Control, Dyn.*, vol. 21, no. 6, pp. 1015–1017, Nov. 1998.

[14] L. Casalino, "Approximate optimization of low-thrust transfers between low-eccentricity close orbits," *J. Guid., Control, Dyn.*, vol. 37, no. 3, pp. 1003–1008, May 2014.

[15] S. Sreesawet and A. Dutta, "Fast and robust computation of low-thrust orbit-raising trajectories," *J. Guid., Control, Dyn.*, vol. 41, no. 9, pp. 1888–1905, Sep. 2018.

[16] D. Wu, F. Jiang, and J. Li, "Warm start for low-thrust trajectory optimization via switched system," *J. Guid., Control, Dyn.*, vol. 44, no. 9, pp. 1700–1706, Sep. 2021.

[17] M. Di Carlo and M. Vasile, "Analytical solutions for low-thrust orbit transfers," *Celestial Mech. Dyn. Astron.*, vol. 133, no. 7, pp. 1–38, Jul. 2021.

[18] G. Avanzini, A. Palmas, and E. Vellutini, "Solution of low-thrust Lambert problem with perturbative expansions of equinoctial elements," *J. Guid., Control, Dyn.*, vol. 38, no. 9, pp. 1585–1601, Sep. 2015.

[19] P. Gurfil, "Analysis of J_2-perturbed motion using mean non-osculating orbital elements," *Celestial Mech. Dyn. Astron.*, vol. 90, no. 3, pp. 289–306, 2004.

[20] M. Cerf, "Low-thrust transfer between circular orbits using natural precession," *J. Guid., Control, Dyn.*, vol. 39, no. 10, pp. 2232–2239, Oct. 2016.

[21] C. Wen, C. Zhang, Y. Cheng, and D. Qiao, "Low-thrust transfer between circular orbits using natural precession and yaw switch steering," *J. Guid., Control, Dyn.*, vol. 44, no. 7, pp. 1371–1378, Jul. 2021.

[22] A.-Y. Huang, Y.-Z. Luo, and H.-N. Li, "Optimization of low-thrust rendezvous between circular orbits via thrust-switch strategy," *J. Guid., Control, Dyn.*, vol. 45, no. 6, pp. 1143–1152, Jun. 2022.

[23] H.-X. Shen, "Explicit approximation for J2-perturbed low-thrust transfers between circular orbits," *J. Guid., Control, Dyn.*, vol. 44, no. 8, pp. 1525–1531, Aug. 2021.

[24] L. Casalino and A. Forestieri, "Approximate optimal LEO transfers with J_2 perturbation and dragsail," *Acta Astronautica*, vol. 192, pp. 379–389, Mar. 2022.

[25] A.-Y. Huang and H.-N. Li, "Simplified optimization model for low-thrust perturbed rendezvous between low-eccentricity orbits," *Adv. Space Res.*, vol. 71, no. 11, pp. 4751–4764, Jun. 2023.

[26] C. Sánchez-Sánchez and D. Izzo, "Real-time optimal control via deep neural networks: Study on landing problems," *J. Guid., Control, Dyn.*, vol. 41, no. 5, pp. 1122–1135, May 2018.

[27] M. Tipaldi, R. Iervolino, and P. R. Massenio, "Reinforcement learning in spacecraft control applications: Advances, prospects, and challenges," *Annu. Rev. Control*, vol. 54, pp. 1–23, 2022.

[28] W. Li, Y. Song, L. Cheng, and S. Gong, "Closed-loop deep neural network optimal control algorithm and error analysis for powered landing under uncertainties," *Astrodynamics*, vol. 7, no. 2, pp. 211–228, Jun. 2023.

[29] L. Cheng, Z. Wang, F. Jiang, and J. Li, "Fast generation of optimal asteroid landing trajectories using deep neural networks," *IEEE Trans. Aerosp. Electron. Syst.*, vol. 56, no. 4, pp. 2642–2655, Aug. 2020.

[30] H. Li, H. Baoyin, and F. Topputo, "Neural networks in time-optimal low-thrust interplanetary transfers," *IEEE Access*, vol. 7, pp. 156413–156419, 2019.

[31] Y.-H. Zhu and Y.-Z. Luo, "Fast approximation of optimal perturbed long-duration impulsive transfers via artificial neural networks," *IEEE Trans. Aerosp. Electron. Syst.*, vol. 57, no. 2, pp. 1123–1138, Apr. 2021.

[32] A. Huang and S. Wu, "Neural network-based approximation model for perturbed orbit rendezvous," *Mathematics*, vol. 10, no. 14, p. 2489, Jul. 2022.

[33] F. Jiang, H. Baoyin, and J. Li, "Practical techniques for low-thrust trajectory optimization with homotopic approach," *J. Guid., Control, Dyn.*, vol. 35, no. 1, pp. 245–258, Jan. 2012.

[34] H. Li, S. Chen, and H. Baoyin, "J_2-perturbed multitarget rendezvous optimization with low thrust," *J. Guid., Control, Dyn.*, vol. 41, no. 3, pp. 802–808, Mar. 2018.

[35] S. Zhao, J. Zhang, K. Xiang, and R. Qi, "Target sequence optimization for multiple debris rendezvous using low thrust based on characteristics of SSO," *Astrodynamics*, vol. 1, no. 1, pp. 85–99, Sep. 2017.

[36] K. Price, R. Storn, and J. Lampinen, *Differential Evolution: A Practical Approach to Global Optimization* (Natural Comput. Series). Berlin, Germany: Springer, 2005.

[37] J. J. Moré, B. S. Garbow, and K. E. Hillstrom, "User guide for MinPack-1," Tech. Rep., Aug. 1980, pp. 59–143.

[38] A. Gulli and S. Pal, *Deep Learning With Keras*. Birmingham, U.K.: Packt Publishing, 2017.

AN-YI HUANG was born in Henan, China, in 1988. He received the Ph.D. degree in aerospace engineering from NUDT, Hunan, China, in 2021. Since December 2020, he has been an Assistant Research Fellow with the State Key Laboratory of Astronautic Dynamics. His research interests include spacecraft dynamics, trajectory optimization, and evolutionary computation.

TIAN-JIAO ZHANG was born in Shaanxi, China, in 1988. She received the Ph.D. degree in aerospace engineering from XJTU, Xi'an, China, in 2018. Her research interests include global optimization and evolutionary computation.